Supplementary Information

Oriented growth of semiconducting TCNQ@$Cu_3(BTC)_2$ MOF on $Cu(OH)_2$: crystallographic orientation and pattern formation toward semiconducting thin-film devices

Kenji Okada,[a, b]* Keyaki Mori,[a] Arisa Fukatsu[a] and Masahide Takahashi[a]*

[a] *Department of Materials Science, Graduate School of Engineering, Osaka Prefecture University, Sakai, Osaka, 599–8531, Japan.* [b] *JST, PRESTO, 4-1-8 Honcho, Kawaguchi, Saitama, 332-0012, Japan.*

Experimental details

Materials

H_3BTC (Benzene-1,3,5-tricarboxylic acid), ethanol (99%) and acetone were purchased from FUJIFILM Wako Pure Chemical Corporation. TCNQ (7,7,8,8-Tetracyanoquinodimethane) were purchased from Tokyo Chemical Industry Co., LTD. All reactants were used without any further purification. Deionized water was used.

Synthesis of $Cu_3(BTC)_2$ oriented film

Oriented $Cu(OH)_2$ nanobelt films on substrates (e.g., round-shaped glass plate, polyimide film or Si wafer) were prepared according to the previously reported method. The conversation from $Cu(OH)_2$ nanobelt to $Cu_3(BTC)_2$ was conducted at room temperature for 10 min by immersing the copper hydroxide nanobelt film in 10 mL of a ethanol (EtOH)-water (H_2O) mixture (1:1 vol.%) containing 7 mg H_3BTC. After 10 min, the product was removed from the solution and washed with ethanol, and then dried under air. This synthesis condition results in the formation of homogeneous and defect-free $Cu_3(BTC)_2$ thin films, as reported in our previous study on the conversion of random copper hydroxide nano-assemblies to $Cu_3(BTC)_2$ coating [K. Okada et al., *CrystEngComm*, 2017, **19**, 4194-4200.].

For the preparation of $Cu_3(BTC)_2$ oriented film for electrical conductivity measurements, Pt pads with 500 nm thick (dimensions 2000 μm by 400 μm) and the gaps of 100, 200 and 500 μm were deposited on oriented a $Cu(OH)_2$ nanobelt film prepared on a polyimide film prior to the conversation from $Cu(OH)_2$ nanobelt to $Cu_3(BTC)_2$.

Fabrication of oriented $Cu_3(BTC)_2$ patterns

The photoresist patterns were fabricated on a Si wafter using a standard UV lithography method. 500W super high pressure mercury lamp, an interference filter at 365 nm, was employed as a UV source (UV Intensity : 8.6 mW/cm^2). A Si wafer was covered with photoresist (Eco UV Resin, Shenzhen Anycubic Technology Co., Ltd., China) by spin coating at 3000 rpm for 40 s. The photoresist coating on a Si wafer was exposed to UV illumination for 15 s through a photo mask with Cr patterns (Edmund Optics). The unilluminated parts were removed by soaling the film into 2-propanol. The $Cu(OH)_2$ oriented thin film was deposited onto the photoresist pattern on the Si wafer (the deposition process is the same as on the flat substrate). The film was then immersed in acetone and sonicated for 10 minutes to remove the photoresist. Then the film was washed with acetone and dried under air. The conversation from $Cu(OH)_2$ nanobelt to $Cu_3(BTC)_2$ was conducted using the same procedure described above.

Infiltration of TCNQ in $Cu_3(BTC)_2$ oriented film

The $Cu_3(BTC)_2$ oriented film prepared on polyimide was placed into a borosilicate glass tube and desolvated under high vacuum (~10^{-4} Pa) at 180 ºC for 3h using a Schlenk line. The film was removed from borosilicate glass tube in a glove bag filled with N_2 gas and immersed in a saturated TCNQ solution in dichloromethane for three days. After three days, the TCNQ@$Cu_3(BTC)_2$ was washed with

dichloromethane twice, and then dried under air.

Characterization

Morphologies of samples were observed by a field-emission scanning electron microscope (FE-SEM: S-4800, Hitachi High-Tech Corporation, Japan) (with electrically conducting metal coating). Crystal phases of the obtained samples were identified by X-ray diffraction (Smart Lab, Rigaku Corporation, Japan) using CuKα radiation (λ = 0.154 nm). The orientation relationship was investigated by azimuthal angle dependence of intensity profiles (φ scan) and in-plane reciprocal space map (RSM). *I-V* curves were recorded between the by contacting the Pt electrodes with microprobes and sweeping the voltage between -10 and 10 V using a parameter analyzer (4200A-SCS, Keithley Instruments, USA). The specific conductivity σ was calculated by the following equation.

$$\sigma = \frac{I}{V} \cdot \frac{l}{w \cdot t}$$

I, V, l, w, and t indicates the measured current, applied voltage, distance between the electrodes, width of the electrodes, and film thickness, respectively. The average film thickness of 300 nm was assumed. A 3D printed base was used to hold and bend the film. The bending test was performed on TCNQ@$Cu_3(BTC)_2$ film on which Pt pads with 100 nm thick deposited. The direction of the electrical measurement was parallel to the {111} lattice planes.

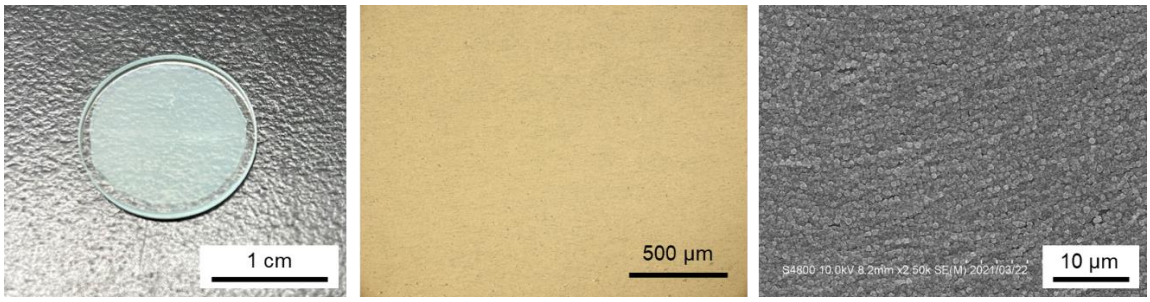

Fig. S1 Large-scale fabrication of the homogeneous oriented $Cu_3(BTC)_2$ thin film.

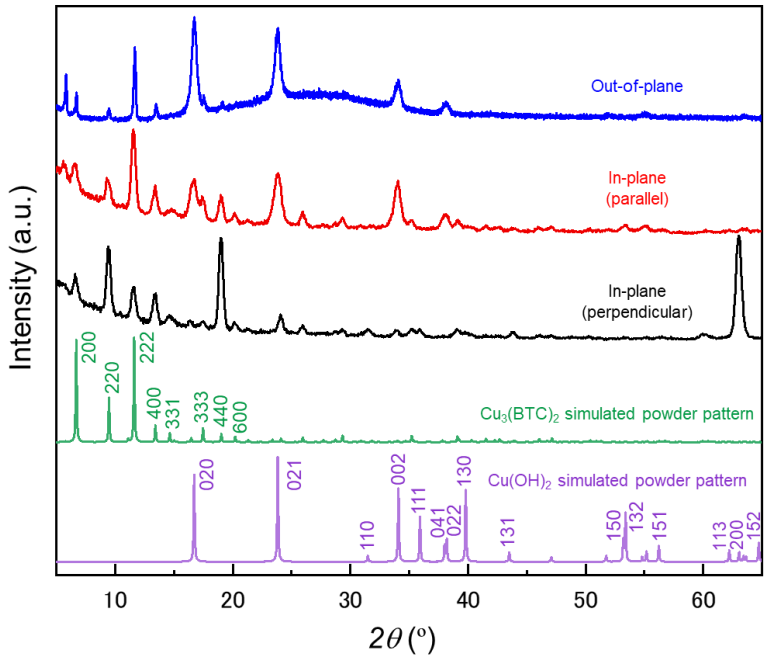

Fig. S2 XRD patterns of the oriented $Cu_3(BTC)_2$ thin film and simulated powder diffraction patterns of $Cu_3(BTC)_2$ and $Cu(OH)_2$. Three setups for the XRD investigations were used for the oriented $Cu_3(BTC)_2$ thin film; out-of-plane (blue line), in-plane (red and black line, X-ray incident angle is parallel and perpendicular to longitudinal direction of nanobelts at $\varphi = 0°$).

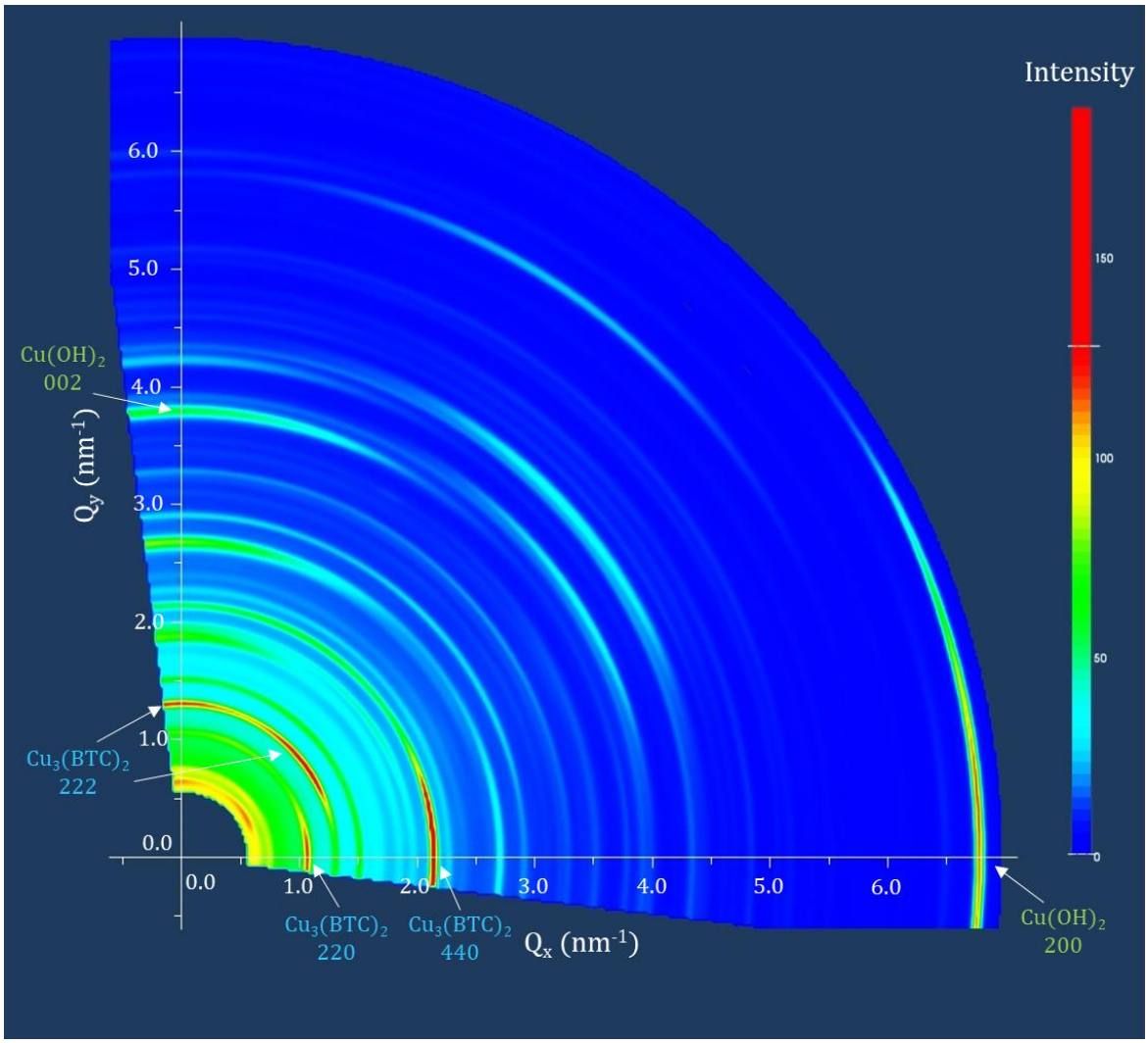

Fig. S3 In-plane RSM of the oriented $Cu_3(BTC)_2$ thin film ($Q = 1/d$, d: lattice spacing). Q_x and Q_y axes are parallel and perpendicular to longitudinal direction (*a* axis) of underlying $Cu(OH)_2$ nanobelts, respectively.

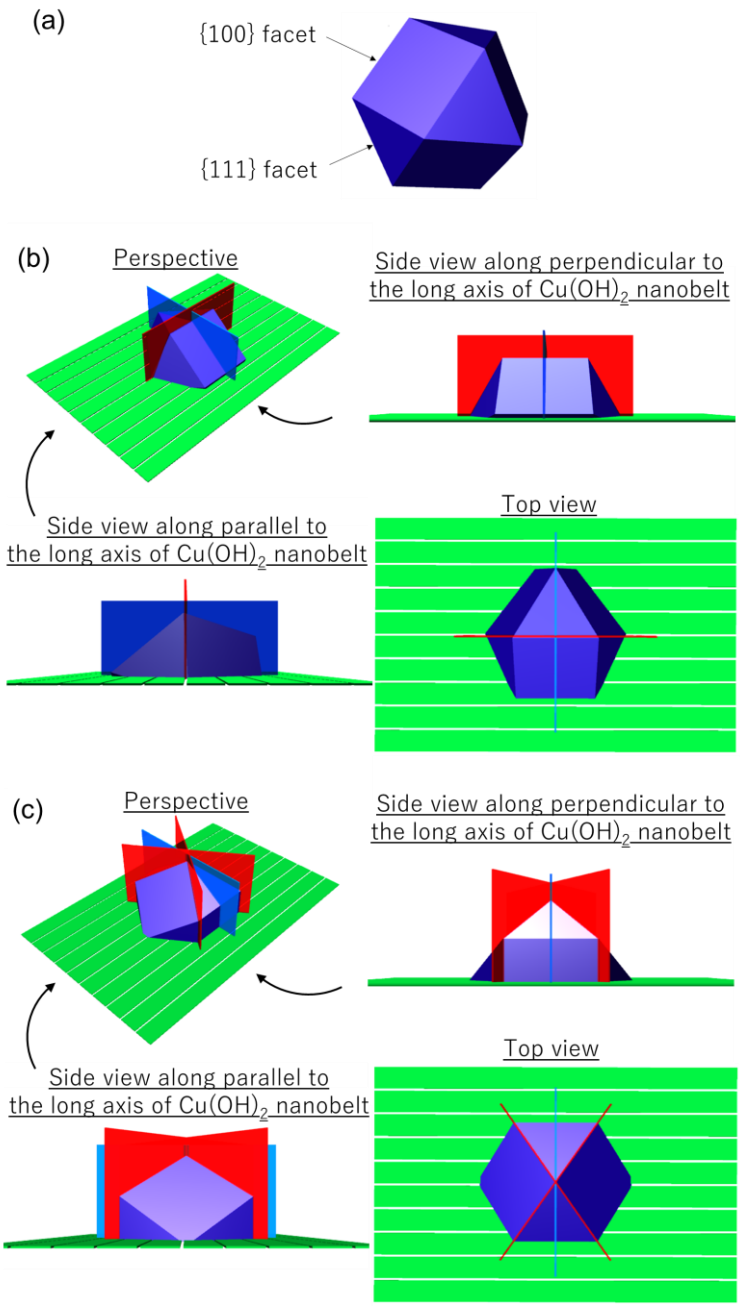

Fig. S4 Schematics of a cuboctahedron-shaped $Cu_3(BTC)_2$ crystal (a) and $Cu_3(BTC)_2$ epitaxially grown under $[\ 11\bar{1}\ ](112)Cu_3(BTC)_2//[001](010)Cu(OH)_2$ (b) and $[001](110)Cu_3(BTC)_2//[001](010)Cu(OH)_2$ (c) orientation relationships. The cuboctahedron-shaped crystals and green rectangles denote $Cu_3(BTC)_2$ crystals and $Cu(OH)_2$ nanobelts, respectively. Only the {111} (red plate) and {110} (blue plate) lattice planes perpendicular to the substrate are shown.

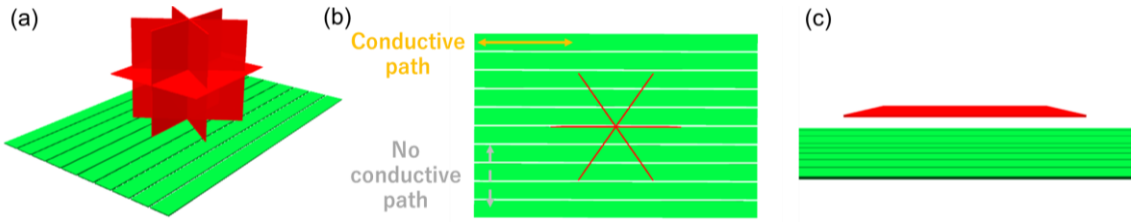

Fig. S5 Schematic illustrations showing the {111} lattice planes (red plates), only parallel and perpendicular to the substrate, in the oriented $Cu_3(BTC)_2$ thin film. $Cu_3(BTC)_2$ crystals are not described to clearly exhibit the directional relationship between the {111} lattice planes and underlying $Cu(OH)_2$ nanobelts. (a) Perspective view of the {111} lattice planes both parallel and perpendicular to the substrate. The green rectangles denote $Cu(OH)_2$ nanobelts (The longitudinal direction coincides with the *a* axis of $Cu(OH)_2$). (b) Top view: only the {111} lattice planes perpendicular to the substrate are shown. The figure shows that there are {111} lattice planes along the longitudinal direction of $Cu(OH)_2$, but not in the short direction. (c) Cross-sectional view: only the {111} lattice plane parallel to the substrate is shown.

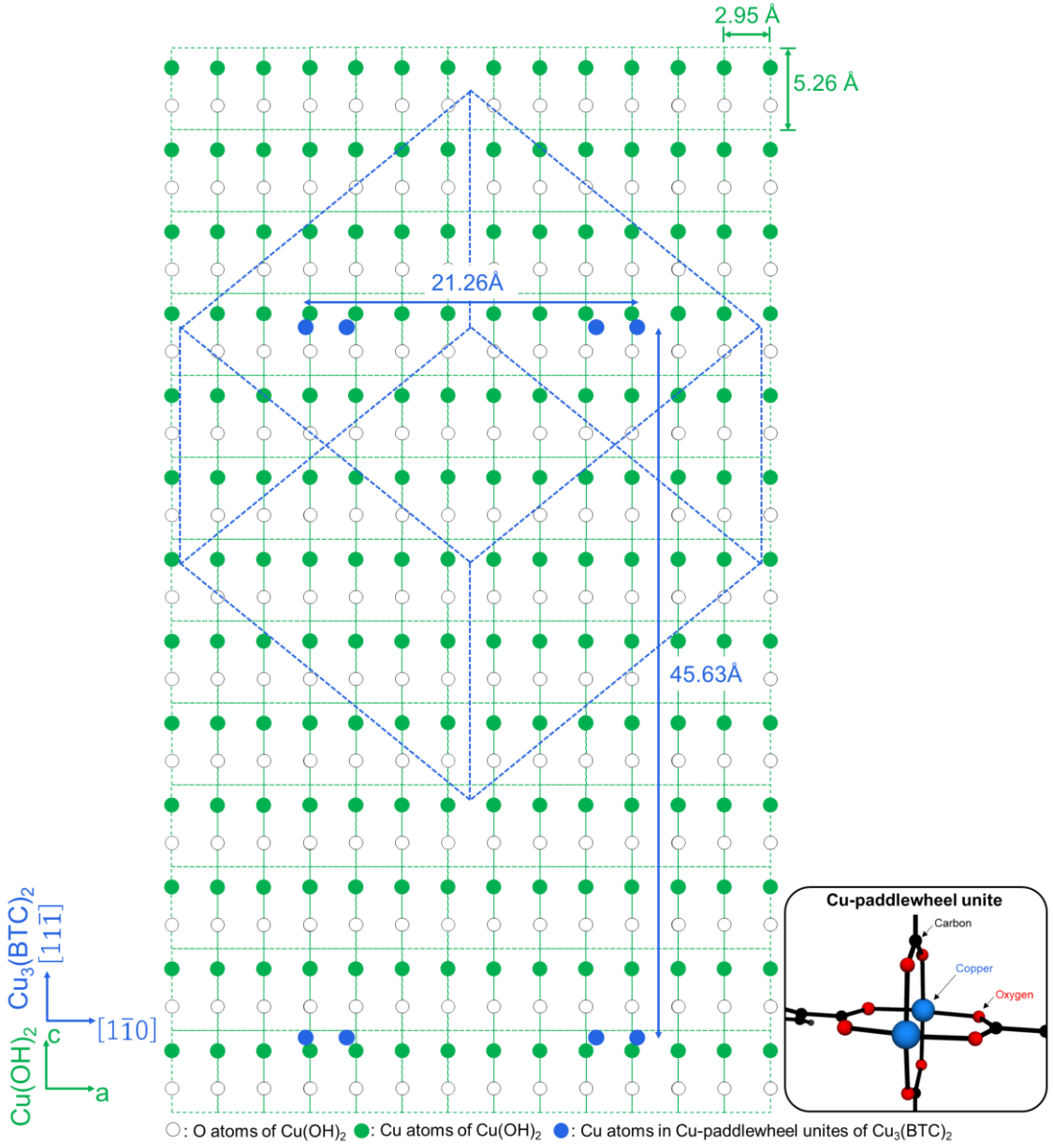

Fig. S6 Schematic illustration showing crystal lattices of $Cu(OH)_2$ and $Cu_3(BTC)_2$ in $[11\bar{1}](112)Cu_3(BTC)_2//[001](010)Cu(OH)_2$ orientation relationship. This illustration corresponds to a crystal structure on the surface of $Cu(OH)_2$ nanobelts. Cu positions are highlighted by different colors for both crystals (green for $Cu(OH)_2$ and blue for $Cu_3(BTC)_2$).

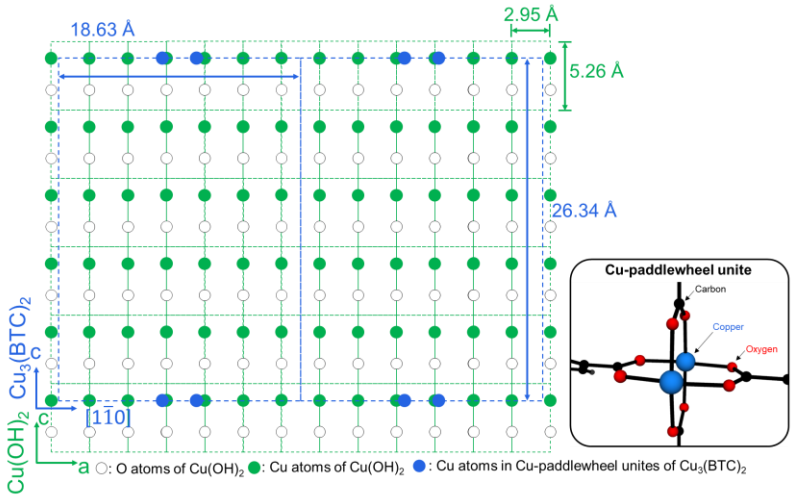

Fig. S7 Schematic illustration showing crystal lattices of $Cu(OH)_2$ and $Cu_3(BTC)_2$ in $[001](110)Cu_3(BTC)_2//[001](010)Cu(OH)_2$ orientation relationship. This illustration corresponds to a crystal structure on the surface of $Cu(OH)_2$ nanobelts. Cu positions are highlighted by different colors for both crystals (green for $Cu(OH)_2$ and blue for $Cu_3(BTC)_2$).

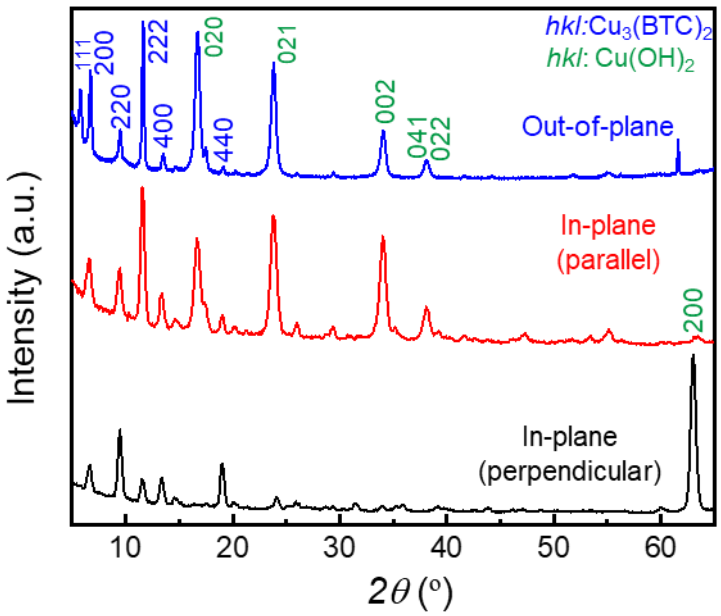

Fig. S8 XRD patterns of the oriented $Cu_3(BTC)_2$ patterns.

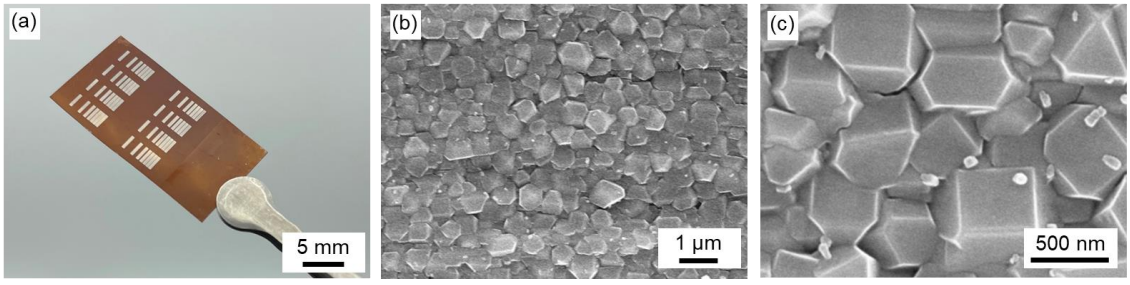

Fig. S9 (a) Photo and (b and c) SEM images of the oriented TCNQ@$Cu_3(BTC)_2$ thin film with Pt electrodes. The small particulate crystals were observed on the surface of $Cu_3(BTC)_2$ crystals after the introduction of TCNQ. This may be CuTCNQ crystals, as similarly observed in the reported papers on TCNQ-introduced $Cu_3(BTC)_2$ (e.g., *Chem. Sci.*, 2018, 9, 7405-7412, *Phys. Chem. Chem. Phys.*, 2019, 21, 25678-25689). The crystals are discrete on the $Cu_3(BTC)_2$ thin film and are not expected to contribute to the conductivity.

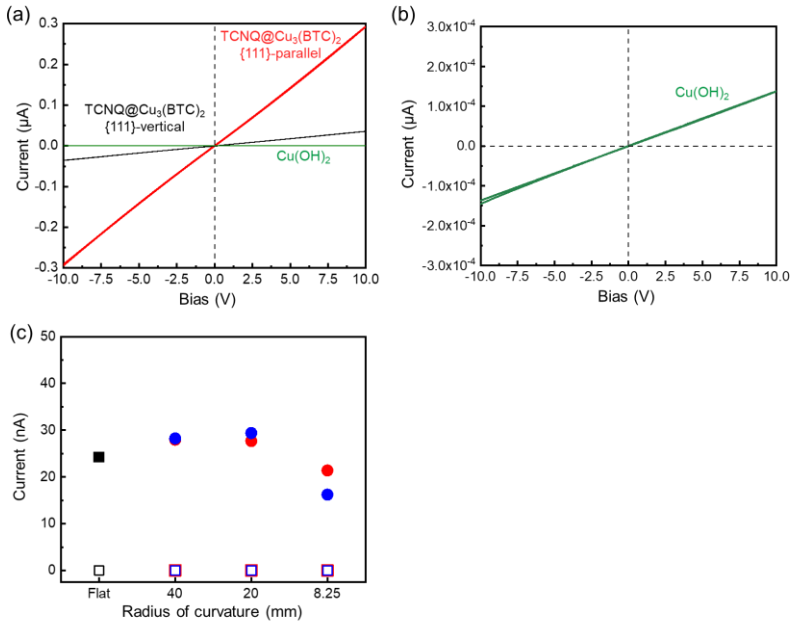

Fig. S10 (a, b) *I-V* curves of the oriented TCNQ@$Cu_3(BTC)_2$ thin films and the $Cu(OH)_2$ nanobelt film on polyimide substrates (Pt pads were 100 μm apart from each other). (c) Current as a function of bending radius of curvature under at 10V (Blue circles (oriented TCNQ@$Cu_3(BTC)_2$ thin film) and squares ($Cu(OH)_2$ nanobelt film): bending of a substrate perpendicular to the longitudinal direction (*a* axis) of underlying $Cu(OH)_2$ nanobelts. Red circles and squares: bending of a substrate perpendicular to the short direction (*c* axis) of underlying $Cu(OH)_2$ nanobelts).

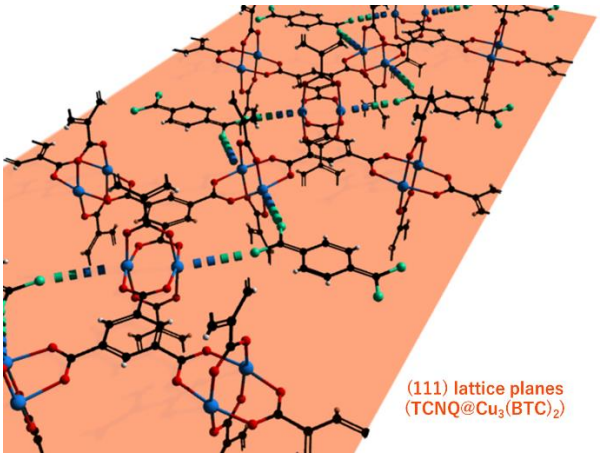

Fig. S11 Schematic illustration of preferential arrangement of TCNQ in the {111} lattice plane (orange tile) of $Cu_3(BTC)_2$ MOF. The TCNQ molecules bind to the apical position of two neighboring Cu paddlewheels. Cu, C, O, and N atoms are denoted in blue, black, red, and green, respectively. This schematic illustration was prepared based on the reported paper, C Schneider et al., *Chem. Sci.*, 2018 ,9, 7405-7412.